agronomy

MDPI

Article

Analysis of Spectral Characteristics of Cotton Leaves at Bud Stage under Different Nitrogen Application Rates

Jiaqiang Wang [1,2,3], Caiyun Yin [4], Weiyang Liu [1,2,3,*], Wenhao Xia [1,2,3] and Songrui Ning [5]

[1] College of Agriculture, Tarim University, Alar 843300, China; wjqzky@taru.edu.cn (J.W.); 120210020@taru.edu.cn (W.X.)
[2] Key Laboratory of Genetic Improvement and Efficient Production for Specialty Crops in Arid Southern Xinjiang of Xinjiang Corps, Tarim University, Alar 843300, China
[3] The Research Center of Oasis Agricultural Resources and Environment in Southern Xinjiang, Tarim University, Alar 843300, China
[4] Agricultural Technology Extension Station of the First Division of Xinjiang Production and Construction Corps, Alar 843300, China; 120050027@taru.edu.cn
[5] State Key Laboratory of Eco-Hydraulics in Northwest Arid Region of China, Xi'an University of Technology, Xi'an 710048, China; ning229@xaut.edu.cn
* Correspondence: lwyzky@163.com

Abstract: Soil salinity affects nutrient uptake by cotton. The cotton bud stage is a very important period in the process of cotton planting and directly affects the yield of cotton. The nutritional status of the bud stage directly affects the reflectance spectra of cotton canopy leaves. Therefore, it is of great significance to nondestructively monitor the nutritional status of the cotton bud stage on salinized soil via spectroscopic techniques and perform corresponding management measures to improve cotton yield. In this study, potted plants with different nitrogen application rates were set up to obtain the reflection spectral curves of cotton bud stage leaves, analyze their spectral characteristics under different nitrogen application rates, and establish spectral estimation models of chlorophyll density. The results are as follows: in the continuum removal spectrum of the cotton bud stage, the lowest point of the absorption valley near 500 nm shifted to the shortwave direction with an increasing nitrogen application rate. The mean reflectance between 765 and 880 nm was significantly different between nitrogen-stressed and nitrogen-unstressed cotton. The average reflectance of the near-infrared band, the absorption valley depths near 500 nm and 675 nm, the first derivative of the 710 nm reflectance, and the second derivatives of the 690 nm and 730 nm reflectance increased with increasing nitrogen application and chlorophyll density, and significant correlations were observed with the chlorophyll density. These parameters were modeled using support vector regression (SVR) and artificial neural network (ANN) methods, two commonly used algorithms in the field of machine learning. The determination coefficients of the three chlorophyll samples via the ANN models were 0.92, 0.77, and 0.94 for the modeling set and 0.77, 0.69, and 0.77 for the verification set. The ratio of quartile to root-mean-square error (RPIQ) of the ANN model was greater than 2.2, and the ratio of the standard error of the measured value to the standard error of the predicted (SEL/SEP) was close to 1, indicating that the chlorophyll density estimation models built based on the ANN algorithm had robust prediction ability. Our model could accurately estimate the leaf chlorophyll density in the cotton bud stage.

Keywords: cotton leaves; spectral characteristics; bud stage; nitrogen application rate

Citation: Wang, J.; Yin, C.; Liu, W.; Xia, W.; Ning, S. Analysis of Spectral Characteristics of Cotton Leaves at Bud Stage under Different Nitrogen Application Rates. *Agronomy* **2024**, *14*, 662. https://doi.org/10.3390/agronomy14040662

Academic Editor: Alberto San Bautista

Received: 23 February 2024
Revised: 18 March 2024
Accepted: 22 March 2024
Published: 25 March 2024

1. Introduction

Cotton is the main cash crop in Xinjiang, where 32.07% of the cultivated land is salinized soil. Too much soil salt will not only affect the absorption of nutrients by cotton but also cause osmotic stress to cells or other harm. Nitrogen is one of the essential mineral elements of crops and an important component of chlorophyll, protein, and nucleic acid

in crops [1,2]. Studies have shown that the chlorophyll content, net photosynthetic rate, stomatal conductance, and transpiration rate of crops gradually increase with the increase in nitrogen application in a certain range of nitrogen levels [3–5].

Spectral analysis of crop leaves was carried out using spectral technology to obtain information on the reflectance and absorptivity of different bands to study the spectral characteristics of crops under different nitrogen application rates as well as the relationship between the crop's nitrogen nutrition status and growth and yield, predict crop nitrogen nutrition status, and optimize nitrogen application rates to improve crop growth and yield [6–8]. The basis of crop nutrition monitoring via hyperspectral technology is to clarify the relationship between crop nitrogen application and spectral and biochemical parameters [9].

The spectral characteristics of cotton leaves are related to the plant growth state, chlorophyll content, leaf area index, and other factors [10]. By analyzing the spectral characteristics of cotton leaves with different nitrogen application rates, the growth state and yield of cotton plants under different nitrogen nutrient states can be predicted, which can provide technical support for cotton production. At present, the study of cotton leaf physiological characteristics via spectral technology has become popular in the cotton research field [11]. The study of the nitrogen application rate and spectral characteristics of cotton mainly focuses on monitoring the cotton growth state via remote sensing and spectral technology, predicting the cotton nutrition status via spectral technology, and optimizing the nitrogen application rate. Wang et al. [12] constructed partial least squares regression (PLSR) and principal component regression (PCR) models by using the hyperspectral data of cotton leaves at the seedling, flowering, initial flowering, full flowering, and boll stages and measured leaf nitrogen content (LNC) and oxidase activity (OA). Their results showed that the accuracy and stability of the PLSR models were significantly higher than those of the PCR models. Moreover, the combination of LNC- and OA-sensitive bands could significantly improve the accuracy and universality of the LNC estimation model. It was also believed that using hyperspectral technology to predict SPAD (Soil and Plant Analyzer Development) values in the process of cotton growth and using precise fertilization management measures were the key to achieving high yields of cotton and improving fertilizer utilization rates [13]. Plot experiments with different nitrogen application rates were performed; cotton leaves at the squaring stage, full budding stage, flowering, boll stage, and boll opening stage were sampled, and spectral tests were carried out. Two modeling methods of the characteristic band and spectral index were used to establish cotton nitrogen estimation models, which showed that the inversion effect of the characteristic band modeling SVR model was better than that of the spectral index [14]. Studies have used dried and ground cotton leaf samples to assess the ability of near-infrared spectroscopy to predict leaf nutrient levels. The results show that NIR spectroscopy has high accuracy in predicting essential elements (N, P, K, Ca, Mg, and S $0.76 \leq R^2 \leq 0.98$) and most trace elements (Fe, Mn, Cu, Mo, B, Cl, and Na $0.64 \leq R^2 \leq 0.81$), and the application of NIR spectroscopy on fresh leaves is also quite accurate [15]. Dedeoglu et al. [16] designed hydroponics experiments on peach trees treated with different contents of nitrogen and constructed nitrogen estimation models with reflectance at 425 nm, 574 nm, 696 nm, and 700 nm. The results showed that the models developed using hyperspectral reflectance could distinguish different nitrogen nutrient states of plants with an accuracy of $\geq$70%. These results provided a theoretical basis for the precise fertilization of cotton. There were also studies on the relationship between cotton spectral characteristics and soil nitrogen content, cotton photosynthetic parameters, cotton plant nutrient content, growth indices, and yield factors under different nitrogen application rates [17–19]. These studies could predict the physiological indices of cotton, optimize the application amount of nitrogen fertilizer, and improve the growth and yield of cotton.

Few studies have studied the spectral changes of cotton leaves in specific growth stages under nitrogen stress in salinized soil drip-irrigated cotton fields [20]. Studying the spectral modeling of cotton leaf nutrition in salinized soil is the key to achieving accurate

fertilization of cotton in southern Xinjiang, China. In this study, the spectral characteristics of cotton leaves in the bud stage of salinized soil drip irrigation cotton fields were studied in order to achieve precise fertilization management of cotton at the bud stage by spectral technology. The bud stage is the period of the fastest growth of cotton nutrition and the most sensitive period with the need for water and fertilizer. The nutrient index of cotton in this period is important to monitor to guide fertilizer management. In this study, hyperspectral technology was used for spectral characteristics analysis of cotton leaves at the bud stage to obtain the spectral reflectances, and the growth and development of cotton bud stage leaves were examined through spectral characteristics to achieve nondestructive health monitoring of the cotton bud stage leaves.

2. Materials and Methods

2.1. Experiment Design

The Agricultural Test Station of Tarim University in Alar City, Xinjiang, China, was selected as the test site (80°45′ E, 40°37′ N). This area is part of the extreme continental arid desert climate of the warm temperate zone and is mainly irrigated. The area where the experimental field is located has an annual precipitation of about 56 mm, an annual evaporation of about 2000 mm, a frost-free period of about 220 days, an annual average temperature of about 10.7 °C, an annual sunshine duration of about 2900 h, and a cumulative temperature greater than 10 °C of about 4113 °C [21].

To study the quantitative relationship between the spectral vegetation index characteristics of cotton leaves and chlorophyll density on salinized soil, different nitrogen rates were applied to the field plot experiment in 2022. The synthesis of photosynthetic pigments can be indirectly affected by controlling the application rate of nitrogen fertilizer [22] so as to obtain the chlorophyll content of crops with different gradients in different test plots. The total area of the experimental plot is 0.33 ha. The basic nutrient status of the surface layer of the experimental field was as follows: available nitrogen, 36.75 mg kg^{-1}; available phosphorus, 10.48 mg kg^{-1}; available potassium, 188.06 mg kg^{-1}; organic matter, 14.15 g kg^{-1}; total salt, 5.62 g kg^{-1}; and pH 8.50. There were 5 treatments with 3 replicates per treatment, and each treatment was 0.02 ha. Drip irrigation under film was used in the experimental plot. Nitrogen application rate of 0 kg·hm^{-2} was used as the reference. Five nitrogen application gradients of 0 kg·hm^{-2} (N0), 150 kg·hm^{-2} (N1), 300 kg·hm^{-2} (N2), 450 kg·hm^{-2} (N3), and 600 kg·hm^{-2} (N4) were set up, and they were set with 3 replicates per treatment; the artificially controllable conditions were strictly controlled to reduce errors (Figure 1). The nitrogen fertilizer applied in the test field was urea. The application method was integrated with water and fertilizer. From N2 to N4, 100 kg hm^{-2} was applied as base fertilizer, and the rest was applied as topdressing 6 times, respectively, at bud stage, initial flowering stage, full flowering stage, full boll stage, and batting stage, according to 10%, 15%, 25%, 25%, 15%, and 10% of the remaining pure nitrogen applied in each treatment.

2.2. Acquisition of the Spectral Data and Plant Sample Collection

The spectral measurements were all carried out in clear and windless weather at the bud stage of cotton with a time interval of 12:00–16:00. An ASD Fieldspec FR2500 spectrometer (Kirkland, WA, USA) was used to measure the spectral reflectance of 350–1050 nm cotton leaves with a spectral resolution of 1 nm. The probe field of view of this spectrometer is 25°, so the measurement height of this study was set to 25 cm. Radiometric correction was performed with a whiteboard before spectral testing. Spectral data and plant samples were collected on 15 June 2022, during the cotton bud stage. In each treatment, spectral reflectance was measured on the functional leaves of 20 sample points. Five cotton plants were selected at each sample point, and five spectral curves were measured, and the average value was used as the average reflectance of the cotton plant. Therefore, a total of 300 spectral reflectance curves were obtained. After obtaining spectral reflectance data of the leaves of 5 cotton plants from each sample point, the corresponding leaves were collected as a mixed sample, and 20 mixed samples were collected for each treatment, for a

total of 300 mixed samples. After the cotton leaf mixed sample was collected, it was put into 0–4 °C incubator and sent to the laboratory to determine the chlorophyll content.

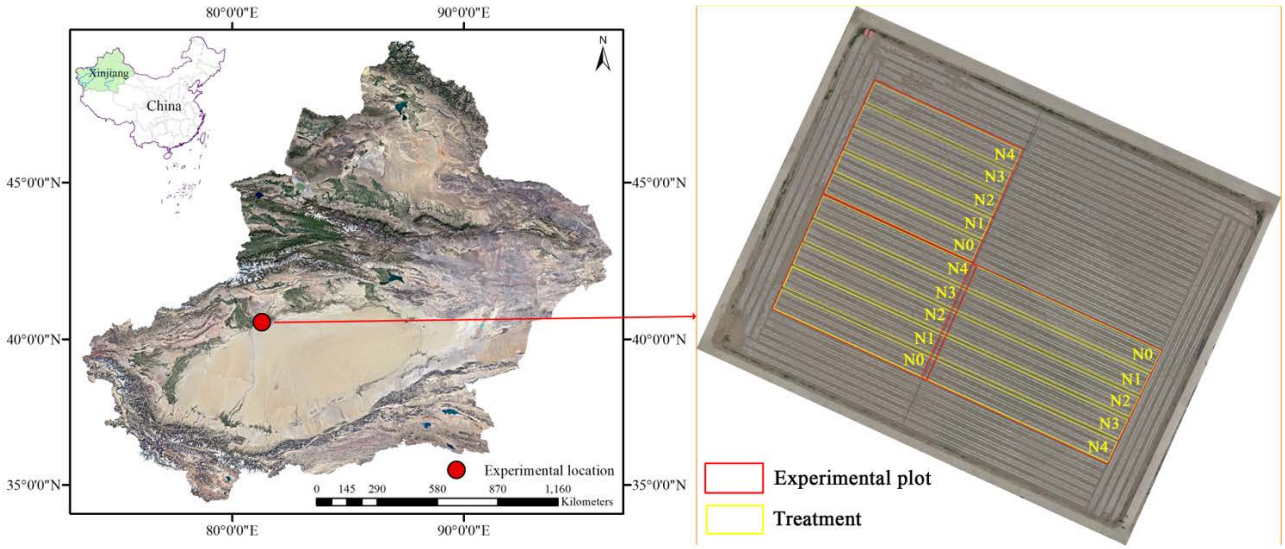

Figure 1. Schematic of the experimental location and experimental design.

2.3. Methods for the Spectral Data Pretreatment

The Savitzky–Golay (SG) filter method was used to smooth and denoise spectral data in the MATLAB 2016a environment. The calculation method of SG convolution smoothing is as follows:

$$X_{i,Savitzky-Golay} = \frac{\sum_{j=-m}^{m} c_j X_{i+j}}{N} \quad (1)$$

where $X_{i,Savitzky-Golay}$ is the value after smoothing at wavelength i; X is the value before smoothing; m is the number of smoothing windows on the wavelength side; N is the normalized index; and $\sum_{j=-m}^{m} c_j X_{i+j}$ is the smoothing coefficient, which is obtained by polynomial fitting [23].

In this study, other spectral transformation methods [24] are as follows:

Continuum removal is calculated as follows:

$$CR_j = \frac{R_j}{RC_j} \quad (2)$$

where CR_j is the spectral reflectance of continuum removal, R_j is the original spectral reflectance, and RC_j is the continuum line reflectance.

The first derivative is calculated as follows:

$$R'_i = \frac{R_{i+1} - R_{i-1}}{2\Delta\lambda} \quad (3)$$

where R'_i is the spectral value of the first derivative, R_{i+1} is the original spectral reflectance of band $i + 1$, R_{i-1} is the original spectral reflectance of band $i - 1$, and $\Delta\lambda$ is the band interval between wavelengths λ_{i+1} and λ_i.

The second derivative is calculated as follows:

$$R''_i = \frac{R'_{i+1} - R'_{i-1}}{2\Delta\lambda} \quad (4)$$

where R''_i is the spectral value of the second derivative, R'_{i+1} is the first derivative value of band $i + 1$, R'_{i-1} is the first derivative value of band $i - 1$, and $\Delta\lambda$ is the band interval between wavelengths λ_{i+1} and λ_i.

2.4. Determination of Chlorophyll Density

The chlorophyll density was extracted via tris-acetone buffer solution and determined via ultraviolet spectrophotometry using the following calculations:

$$C_a \left(\mu\text{mol mL}^{-1}\right) = 0.01373A_{663} - 0.000897A_{537} - 0.003046A_{647} \quad (5)$$

$$C_b \left(\mu\text{mol mL}^{-1}\right) = 0.02405A_{647} - 0.0004305A_{537} - 0.005507A_{663} \quad (6)$$

$$Chl\ a \left(\text{mg m}^{-2}\right) = C_a \times M_a \times V/(1000 \times W_F \times SLW) \quad (7)$$

$$Chl\ b \left(\text{mg m}^{-2}\right) = C_b \times M_b \times V/(1000 \times W_F \times SLW) \quad (8)$$

$$Chl\ a+b \left(\text{mg m}^{-2}\right) = Chl\ a + Chl\ b \quad (9)$$

where C_a and C_b are the molar concentrations of chlorophyll a and chlorophyll b, respectively; *Chl a*, *Chl b*, and *Chl a* + *b* are the densities of chlorophyll a, chlorophyll b, and total chlorophyll, respectively; A is absorbance; V is the colorimetric volume; M_a and M_b are the molecular weights of chlorophyll a and chlorophyll b, respectively; W_F is fresh leaf weight; and SLW is the specific leaf weight [25].

2.5. Modeling and Accuracy Verification Methods

Two modeling methods were used to estimate chlorophyll density in this study, namely, the artificial neural network (ANN) algorithm and support vector regression (SVR). These two machine learning algorithms are the most common modeling methods at present [26]. In this study, chlorophyll density is the dependent variable y, and spectral variable is the independent variable x. ANN's multilayer perceptron (MLP) model was used for modeling; the selected kernel function of SVR was polynomial, the regression precision ε was 0.1, penalty parameter C was 6, and the γ value was 2.0.

In this study, R^2, RMSE, RPIQ, and SEL/SEP were used as precision verification parameters [27]. R^2 is the determination coefficient of the model. RMSE is the root mean square error. RPIQ is the ratio of the quartile distance to the RMSE. SEL/SEP is the ratio of the standard error of the measured value to the standard error of the predicted value. The closer that R^2 and SEL/SEP are to 1 and a smaller RMSE correlate to a smaller deviation between the measured value and the predicted value of the index and a higher accuracy of the model. Moreover, it is generally believed that if RPIQ < 1.7, the reliability of the model is low. If 1.7 $\leq$ RPIQ < 2.2, the model has relatively balanced forecasting ability. If RPIQ $\geq$ 2.2, the model has good predictive ability.

3. Results

3.1. Variation Characteristics of Chlorophyll Density in Cotton Leaves at the Bud Stage

The densities of Chl a, Chl b, and Chl a + b in cotton leaves of different treatments at the bud stage were measured, and descriptive statistics were performed for these data (Table 1).

As shown in Table 1, within each treatment, the standard deviation and variance of chlorophyll Chl a, Chl b, Chl a + b, and Chl a/Chl b values were low. From the perspective of maximum and minimum values, the data in these groups were relatively concentrated with a small degree of dispersion. From the perspective of standard error, the sampling distribution and sampling error of the data were relatively low. Therefore, the samples remained highly representative, and the data were relatively reliable. The coefficient of variation (C. V.) could reflect the variation in chlorophyll density in cotton leaves within the group. Usually, a CV $\leq$ 10% represents weak variation, 10% $\leq$ CV $\leq$ 100% represents medium variation, and CV $\geq$ 100% represents strong variation (Kesteven, 1946) [28]. The maximum variation coefficient of all chlorophyll densities was 26.67. Therefore, the

chlorophyll densities (Chl a, Chl b, Chl a + b, Chl a/Chl b) of all treatments were in the degree of weak and medium variation.

Table 1. Descriptive statistics of leaf chlorophyll density at the cotton bud stage.

Type	Treatment	Minimum	Maximum	Mean	S.D.	SEM.	VAR.	C.V.
Chl a	N0	0.21	0.49	0.15	0.04	0.02	0.001	26.67
	N1	0.35	0.57	0.28	0.06	0.03	0.004	21.43
	N2	0.34	0.39	0.29	0.06	0.03	0.004	20.69
	N3	0.38	0.38	0.36	0.01	0.01	0.000	2.78
	N4	0.41	0.45	0.38	0.03	0.02	0.001	7.89
Chl b	N0	0.07	0.10	0.08	0.01	0.01	0.000	12.50
	N1	0.09	0.14	0.11	0.02	0.01	0.000	18.18
	N2	0.08	0.14	0.12	0.02	0.01	0.001	16.67
	N3	0.14	0.15	0.15	0.01	0.00	0.000	6.67
	N4	0.14	0.16	0.15	0.01	0.00	0.000	6.67
Chl a + b	N0	0.19	0.32	0.24	0.05	0.02	0.002	20.83
	N1	0.27	0.49	0.39	0.08	0.04	0.007	20.51
	N2	0.29	0.48	0.41	0.08	0.04	0.006	19.51
	N3	0.49	0.53	0.51	0.02	0.01	0.000	3.92
	N4	0.49	0.57	0.53	0.04	0.02	0.001	7.55
Chl a/Chl b	N0	1.71	2.05	1.85	0.12	0.05	0.015	6.48
	N1	2.07	2.66	2.41	0.23	0.10	0.053	9.54
	N2	2.12	2.98	2.48	0.33	0.15	0.107	13.31
	N3	2.30	2.54	2.47	0.11	0.06	0.013	4.45
	N4	2.39	2.68	2.48	0.14	0.07	0.018	5.65

Note: Chl a, Chl b, Chl a + b, and Chl a/Chl b are chlorophyll a density, chlorophyll b density, total chlorophyll density, and ratio of chlorophyll a to chlorophyll b, respectively. S.D., SEM., VAR and C.V. are standard deviation, standard error, variance and coefficient of variation respectively.

The cotton in the bud stage was mainly in a vegetative growth stage. Some differences were observed in chlorophyll density among the treatments. Under nitrogen stress, the chlorophyll concentration and photosynthetic rate of plant leaves significantly decreased, and plant growth was inhibited [29,30]. The chlorophyll densities (Chl a, Chl b, Chl a + b) of treatment N0 were the lowest, and the analysis of variance showed that the chlorophyll density of treatment N0 was significantly different from those of the other treatments ($p < 0.05$). Since N0 was the no-nitrogen fertilizer treatment, cotton had evident nitrogen stress. The amount of chlorophyll synthesis in the cotton leaves under N0 was insufficient, and led to its chlorophyll density always being at a low level, which was far lower than those of other treatments. This may result in lower photosynthetic intensity and inadequate plant nutrients supplied to unfertilized cotton leaves.

The amount of conventional pure nitrogen application is 300 kg·hm^{-2} in the cotton planting area of Xinjiang [31]. Treatment N1 represents half of the traditional amount of nitrogen application, and treatment N2 represents the traditional amount of nitrogen application, respectively. Table 1 shows that the chlorophyll densities of N1 and N2 were higher than that of N0 and lower than that of N3 and N4. The analysis of variance showed that there were no significant differences in the chlorophyll densities of N1 and N2 ($p > 0.05$), but they were significantly lower than those of N3 and N4 ($p \leq 0.05$). It was indicated that the chlorophyll density of cotton leaves could reach the same level with 0.5 times the conventional application rate compared with that of the conventional application amount in the cotton planting area of Xinjiang. While the difference in chlorophyll density between N3 and N4 was not significant ($p > 0.05$), it was significantly higher than the chlorophyll density of other treatments ($p \leq 0.05$). It was also indicated that the chlorophyll density of cotton leaves significantly increased when the nitrogen application was more than conventional. Further, 1.5 times and 2 times the amount of conventional fertilization had the same effect. From the measured net photosynthetic rate, the values of N0 to N4 were 27.2 μmol CO_2 m^{-2} s^{-1}, 28.0 μmol CO_2 m^{-2}s^{-1}, 22.5 μmol CO_2 m^{-2}s^{-1},

19.4 μmol CO_2 m^{-2} s^{-1}, and 17.2 μmol CO_2 $m^{-2}s^{-1}$, respectively. N3 and N4 were significantly higher than other treatments. Specifically, the chlorophyll densities of the leaves of cotton grown on the basis of the two fertilization amounts were not significantly different, but their photosynthetic intensities and plant nutrient status were significantly better than those of the other treatments. The Chl a/Chl b value of N0 was significantly lower than those of other treatments ($p \leq 0.05$), and the differences among other treatments were not significant ($p > 0.05$). It was indicated that nitrogen stress occurred for the cotton without fertilization treatment, and its physiological function had been affected. Because it is a healthy plant, the ratio of Chl a to Chl b was constant [32]. In this study, the ratio of chl a to chl b of cotton leaves at bud stage was about 2.5 (Table 1). A significant change in the Chl a/Chl b value occurred, illustrating that the physiological function was affected. Therefore, in Table 1, with the exception of N0, no nutrient stress occurred for the cotton of other treatments, and their physiological functions remained at a healthy level.

3.2. The Spectral Characteristics of Cotton Leaves at the Bud Stage

The spectral reflectance of cotton leaves at 350~1050 nm was measured under different treatments. The reflectance curves were smoothed, and then continuum removal was carried out. Moreover, the reflectivity spectrum curves were resampled at 10 nm, and the first- and second-order differential treatments were performed to analyze the spectral characteristics of the cotton leaves at the bud stage.

Under nitrogen deficiency, the substrate area of plant leaf chloroplasts becomes larger, the lamellar structure is loose, and the gap is serious [33]. Figure 2a shows that all the original reflectance spectra curves of cotton leaves at the bud stage were consistent with those of typical green plants. Moreover, all the reflectance peaks occurred in the green band at approximately 550 nm and the near-infrared band between 750 nm and 1050 nm. Two absorption valleys were observed in the blue–violet band at approximately 410 nm and the red band at approximately 670 nm. The reflectance spectrum curve of vegetation sharply increased in the red-edge band of 680–760 nm, forming a steep and nearly straight-line shape. In the plateau area of the near-infrared waveband, the reflectivities of cotton leaves at the bud stage of different treatments were significantly different. In the stable region from 765 nm to 880 nm, the average reflectivities of N0, N1, N2, N3, and N4 were 0.265, 0.366, 0.379, 0.446, and 0.470, respectively. Multiple comparisons showed that there were significant differences in leaf reflectance between N0 and the other treatments ($p \leq 0.05$), no significant differences between N1 and N2 ($p \geq 0.05$), significant differences between N1 and N2 with the other treatments ($p \leq 0.05$), no significant differences between N3 and N4 ($p \geq 0.05$), and significant differences between and N3 and N4 with the other treatments ($p \leq 0.05$). The size of the near-infrared spectral reflectance was related to the tissue structure of the cotton leaves at the bud stage of each treatment. Certain differences were apparent in the tissue structure of cotton leaves at the bud stage with the different nitrogen application levels. The spectral reflectance of nitrogen-deficient cotton leaves was low in this band range due to abnormal tissue structure development. However, in the treatments with 1.5 times and 2 times the conventional fertilizer amount, the leaf tissue structure was very healthy, and the spectral reflectance was at a high level in this band range. The wavelength positions of the spectral curves of each treatment reaching the plateau area were not significantly different ($p > 0.5$), which were all approximately 763 nm.

Figure 2b shows the continuum removal spectral curves of the five treatments of cotton leaves at the bud stage, reflecting the spectral absorption characteristics of cotton leaves. As shown in Figure 2b, there were two absorption valleys in the continuum removal curve of leaves, which were located at wavelengths of 500 nm and 675 nm. In these two absorption valleys, the absorption depth of N0 was the lowest, while the absorption depth of N4 was the largest. In the absorption valley near 500 nm, the leaf spectral absorption depth of the N0 treatment was 0.597, which was significantly different from those of the other treatments ($p \leq 0.05$). There was no significant difference between N1 and N2 ($p > 0.5$), and the absorption depths of N1 and N2 were 0.676 and 0.677, respectively; however, they

were significantly different from those of N3 and N4 ($p \leq 0.05$). No significant difference was observed between N3 and N4 ($p > 0.5$), and their absorption depths were 0.719 and 0.723, respectively. No significant difference was observed in the lowest point wavelength of the absorption valley of N1, N2, and N3 ($p > 0.5$), and their values were 500 nm, 502 nm, and 502 nm, respectively, but there was a significant difference between N1, N2, and N3 (495 nm) and N4 (497 nm) ($p \leq 0.05$). In the absorption valley near 675 nm, the leaf spectral absorption depth of the N0 treatment was 0.775, which was significantly different from those of the other treatments ($p \leq 0.05$), and no significant differences were observed between the other treatments ($p > 0.5$). The values of N1 to N4 were 0.825, 0.838, 0.852, and 0.854, respectively. The absorption depth also showed an increasing trend. The lowest point wavelengths of the absorption valley were 675 nm, 674 nm, 676 nm, 677 nm, and 677 nm. No significant differences were observed between the different treatments ($p > 0.5$). Therefore, these two absorption valleys were within the visible light range, and the depth of the absorption valleys near 675 nm was greater than that near 500 nm. However, the lowest point of the absorption valley near 500 nm shifted to the shortwave direction with increasing nitrogen.

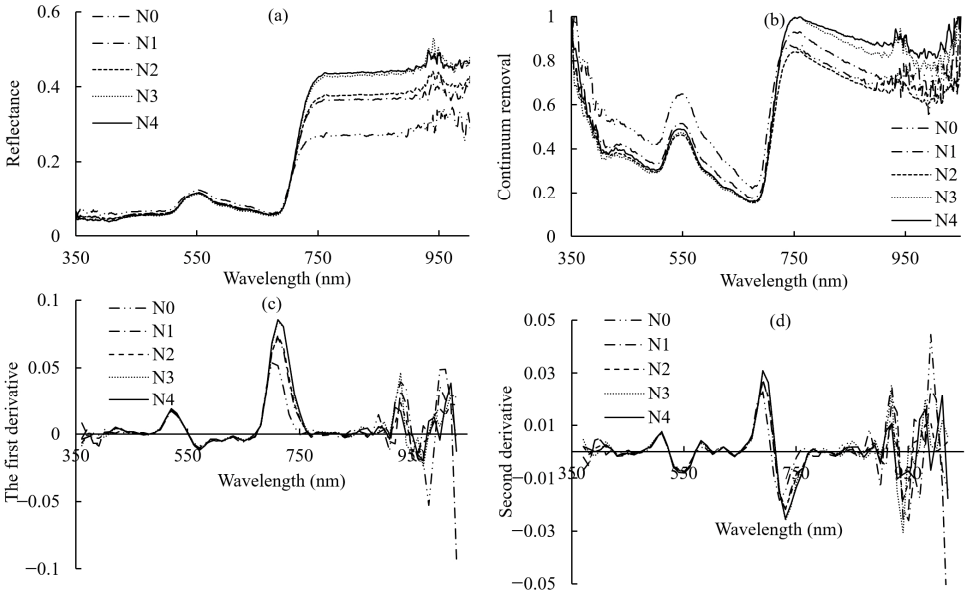

Figure 2. Spectral characteristic curves of cotton leaves at the bud stage under different nitrogen application levels. (**a**) Original reflectance spectral curve, (**b**) Continuum removal spectrum curve, (**c**) The first-derivative spectrum, and (**d**) The second-derivative spectrum.

To show the essential characteristics of the plant spectrum, spectral differentiation technology can be applied to reduce the influence of the noise spectrum on the target ground object spectrum to a certain extent for environmental background and atmospheric effects [34]. Spectral differential data are widely used in the extraction of vegetation biochemical information. In this study, two stable peaks were observed (Figure 2c) in the first-order differential spectral curve of cotton leaves at the bud stage: one at approximately 520 nm and the other at approximately 710 nm. The first-order differential values of each treatment near 520 nm were all approximately 0.188, with no significant difference ($p > 0.5$), forming an almost overlapping peak. For the first-order differential values near 710 nm, no significant difference between the other treatments was observed, except for the significant difference between N0 and other treatments; the first-order differential peak of the treatment N0 appeared at 700 nm, and for all other treatments, the peak appeared after 710 nm. The second-order differential spectrum curve had an evident peak and an evident valley. No significant difference was observed in the second-order differential peak value and the wavelengths of the peak value at approximately 690 nm among all treatments ($p > 0.5$). However, no significant difference was observed in the second-order differential

valley value and the wavelengths of the valley value near 730 nm among all treatments, except for the significant difference between N0 and the other treatments. The valley value of N0 was significantly higher than that of the other treatments, and the valley value appeared at 720 nm, while those of the other treatments appeared at 730 nm. Therefore, the leaf reflectance at approximately 520 nm and 690 nm was not sensitive to changes in the amount of nitrogen application. The leaf reflectance near 710 nm and 730 nm was relatively sensitive to changes in the amount of nitrogen application.

Prsa et al. [35] showed that the chlorophyll content of plant leaves increased with increasing nitrogen application in a certain period. As shown in Figure 3, no significant difference was observed in the mean spectral reflectance of the near-infrared bands (Figure 3a) and the absorption valley spectral absorption depth (Figure 3b) near 500 nm of cotton leaves in the bud stage between N1 and N2 or between N3 and N4. Their values had a significant upward trend with increasing nitrogen application. The absorption depth near 675 nm, the first-order differential peak value (Figure 3c) at 710 nm, and the second-order differential valley value (Figure 3d) at 730 nm of the cotton leaves in treatment N0 were significantly different from those of other treatments, while no significant difference was observed in all other treatments. However, their values also tended to increase with increasing nitrogen application. No significant difference was observed in the second-order differential peak value near 690 nm among all treatments, but a certain increasing trend occurred with increasing nitrogen application. Therefore, the mean spectral reflectance of the near-infrared band, the spectral absorption depth of the absorption valleys near 500 nm and 675 nm, the first-order differential peak near 710 nm, the second-order differential peak near 690 nm, and the second-order differential valley near 730 nm of cotton leaves with different treatments all had an increasing trend. As shown in Figure 3, these spectral transformation values were consistent with the changing trend of chlorophyll density (Chl a, Chl b, Chl a + b); specifically, with the increase in the nitrogen application, the leaf chlorophyll density increased, and the spectral transformation values of some bands of cotton leaves also changed accordingly at the bud stage.

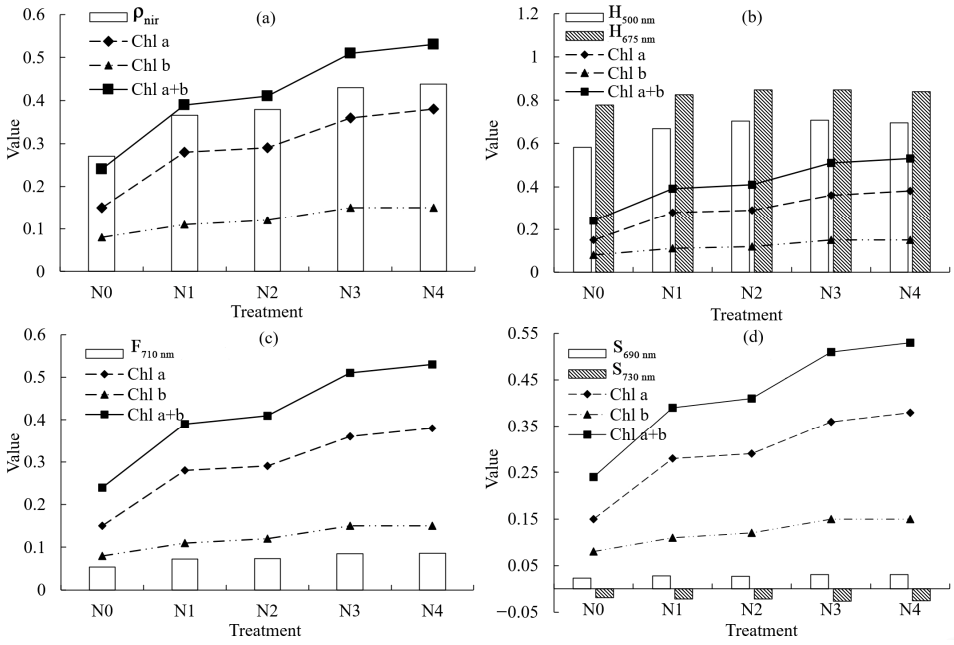

Figure 3. Variation trend of cotton leaf chlorophyll density and different spectral transformation values at the bud stage. (**a**) Variation trend of the near-infrared band average reflectance and chlorophyll density, (**b**) Variation trend of the absorption valley depth at approximately 500 nm and 675 nm and chlorophyll density, (**c**) Variation trend of the first derivative value at approximately 710 nm and chlorophyll density, and (**d**) Variation trend of the second derivative value at approximately 690 nm and 730 nm and chlorophyll density.

Based on the correlation analysis between spectral transformation values and chlorophyll density and the ratio of chlorophyll a to chlorophyll b of cotton leaves at the bud stage (Table 2), a very significant correlation was observed between Chl a, Chl b, Chl a + b and ρ_{nir}, H_{500nm}, H_{675nm}, F_{710nm}, λ_{710nm}, S_{730nm}, and λ_{730nm}. Among them, ρ_{nir}, λ_{710nm}, and S_{730nm} had the greatest correlation. However, the leaf Chl a/Chl b had a very significant correlation with ρ_{nir}, F_{710nm}, λ_{710nm}, S_{730nm}, and λ_{730nm}, and the correlation was the most significant with ρ_{nir}, λ_{710nm}, and λ_{730nm}. Therefore, an estimation of the four kinds of chlorophyll density using these parameters should be possible.

Table 2. Correlation between the spectral transformation values and chlorophyll density and the ratio of chlorophyll a to chlorophyll b in cotton leaves at the bud stage.

Spectral Variables	Chl a	Chl b	Chl a + b	Chl a/Chl b
ρ_{nir}	0.724 **	0.664 **	0.715 **	0.657 **
λ_{nir}	−0.100	−0.053	−0.089	−0.265
H_{500nm}	0.558 **	0.583 **	0.591 **	0.430 *
λ_{500nm}	−0.335	−0.385	−0.350	−0.092
H_{675nm}	0.566 **	0.645 **	0.658 **	0.480 *
λ_{675nm}	0.163	0.288	0.194	−0.078
F_{710nm}	0.694 **	0.673 **	0.694 **	0.536 **
λ_{F710nm}	0.792 **	0.634 **	0.711 **	0.795 **
S_{690nm}	0.525 *	0.506 *	0.524 *	0.387
λ_{S690nm}	0.369	0.361	0.370	0.352
S_{730nm}	−0.696 **	−0.671 **	−0.695 **	−0.558 **
λ_{S730nm}	0.669 **	0.597 **	0.656 **	0.697 **

Note: * means significant correlation; ** means extremely significant correlation; ρ_{nir} is average reflectance in near-infrared band; λ_{nir} is the wavelength position reaching the platform region; H_{500nm} is the depth of the absorption valley near the 500 nm wavelength; λ_{500nm} is the lowest position of the absorption valley near the 500 nm wavelength; H_{675nm} is the depth of the absorption valley near the 675 nm wavelength; λ_{675nm} is the lowest position of the absorption valley near the 675 nm wavelength; F_{710nm} is the maximum of the first derivative near 710 nm. λ_{F710nm} is the wavelength position corresponding to the maximum of the first derivative near 710 nm; S_{690nm} is the maximum of the second derivative near 690 nm; λ_{S690nm} is the wavelength position corresponding to the maximum of the second derivative near 690 nm; S_{730nm} is the minimum of the second derivative near 730 nm; and λ_{S730nm} is the wavelength position corresponding to the minimum of the second derivative near 730 nm. Chl a, Chl b, Chl a + b, and Chl a/Chl b are chlorophyll a density, chlorophyll b density, total chlorophyll density, and ratio of chlorophyll a to chlorophyll b, respectively.

3.3. Chlorophyll Estimation Modeling of Cotton Leaves Based on Spectral Variables

The chlorophyll density data of cotton leaves used for modeling were statistically analyzed. Table 3 shows the descriptive statistical characteristics of the chlorophyll density in the cotton leaves. The average chlorophyll density in the leaves of the whole sample in this study was 6.73 mg m^{-2}. The mean values of the modeling set and validation set were 6.84 mg m^{-2} and 6.38 mg m^{-2}, respectively, and the mean values of the whole sample were between the modeling set and validation set.

Table 3. Statistical characteristics of the chlorophyll density of cotton leaf samples.

Type of Samples	Chlorophyll Type	Sample Number	Maximum	Minimum	Mean	Standard Deviation
Whole sets	Chl a	87	0.45	0.12	0.31	0.08
	Chl b	87	0.16	0.067	0.11	0.03
	Chl a + b	87	0.62	0.19	0.42	0.10
Calibration sets	Chl a	51	0.45	0.14	0.30	0.08
	Chl b	51	0.16	0.07	0.11	0.03
	Chl a + b	51	0.62	0.22	0.41	0.11
Validation sets	Chl a	26	0.42	0.12	0.33	0.08
	Chl b	26	0.15	0.07	0.12	0.02
	Chl a + b	26	0.57	0.19	0.44	0.10

Note: Chl a, Chl b, and Chl a + b are chlorophyll a density, chlorophyll b density, and total chlorophyll density, respectively.

With 12 spectral indices as independent variables and 4 chlorophyll density data as response variables, cotton leaf chlorophyll estimation models based on SVR and ANN algorithms were constructed, and their accuracy was verified.

The spectral parameters in Table 4 were selected to estimate the chlorophyll density of cotton leaves. Spectral parameters were taken as independent variables, and leaf chlorophyll density was taken as the dependent variable. SVR and ANN algorithms were used to estimate leaf chlorophyll density. By comparing the coefficient of determination (R^2), root mean square error (RMSE), the ratio of quartile distance to root mean square error (RPIQ), and the ratio of the standard error of the measured value to the standard error of predicted value (SEL/SEP) between the two models, the optimal models were selected to study the estimation of cotton leaf chlorophyll density at the bud stage under Xinjiang irrigation conditions. R^2 was used to determine the goodness of fit of the models, and RMSE, RPIQ, and SEL/SEP were used to test the reliability of the estimated models.

Table 4. Estimation results of the chlorophyll density in the cotton leaves.

Modeling Method	Chlorophyll Type	Modeling				Verification			
		R^2	RMSE	RPIQ	SEL/SEP	R^2	RMSE	RPIQ	SEL/SEP
SVR	Chl a	0.76	0.07	0.29	5.51	0.66	0.06	0.31	6.61
	Chl b	0.62	0.018	0.86	2.38	0.67	0.016	0.87	2.59
	Chl a + b	0.74	0.093	0.24	6.63	0.66	0.084	0.25	7.85
ANN	Chl a	0.92	0.025	4.13	0.94	0.77	0.050	1.91	0.97
	Chl b	0.77	0.012	3.38	1.17	0.69	0.013	3.12	1.01
	Chl a + b	0.94	0.026	5.77	1.02	0.77	0.050	2.25	1.15

Note: Chl a, Chl b, and Chl a + b are chlorophyll a density, chlorophyll b density, and total chlorophyll density, respectively.

The spectral estimation model of chlorophyll density was established via SVR and ANN algorithms. By comparing the parameters of the different estimation models, the estimation model constructed via the ANN algorithm had higher accuracy, while the model constructed via the SVR algorithm did not pass accuracy verification and could not accurately predict the density of the three kinds of chlorophyll (Figure 4). The determination coefficients of the three chlorophyll samples via the ANN models were 0.92, 0.77, and 0.94 for the modeling set and 0.77, 0.69, and 0.77 for the verification set. In addition, the RPIQ of the ANN model was greater than 2.2, and SEL/SEP was close to 1, indicating that the chlorophyll density estimation models built based on the ANN algorithm had robust prediction ability.

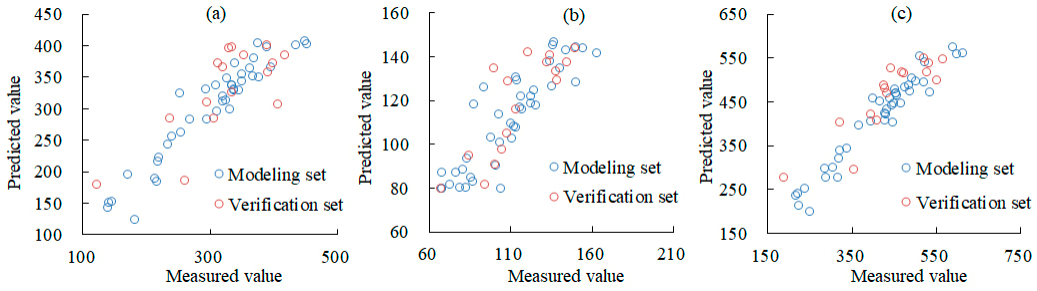

Figure 4. Scatter plots of the predicted and measured chlorophyll density of cotton leaves at the bud stage using the SVM regression model. (**a**) Chl a model, (**b**) Chl b model, (**c**) Chl a + b model.

4. Discussion

4.1. Effects of the Nitrogen Application Rate on the Spectral Characteristics of Cotton Leaves

Nitrogen is an essential nutrient element for crop growth and plays an important role in the process of crop growth. Nitrogen deficiency in crops leads to decreased photosynthesis of plant leaves and growth retardation [36,37]. However, excessive application of

nitrogen fertilizer reduces the tillering of crops [38]. The biological basis of monitoring crop growth via hyperspectral technology is that the difference in the internal structure and material content of crop leaves leads to a difference in spectral reflectivity, and then information on the material composition and internal structure of leaves can be obtained by studying the difference in spectral reflectance. The nitrogen application rate affects some physiological indices of crops and thus affects the spectral characteristics of crops. The spectral characteristics of crops change due to changes in the physiological indices of crops. In this study, chlorophyll density increased with increasing nitrogen application in a certain range. Seven spectral parameters varied with the chlorophyll density of cotton leaves. Studies have shown that the net photosynthetic rate (Pn) and photosynthetically active radiation (FAPAR) of crops are sensitive to changes in nitrogen application. By establishing the relationship between these two factors and hyperspectral data, the band positions sensitive to nitrogen changes are 350–450 nm and 600–750 nm [39]. The above deductions are related to the conclusions of this study. A high correlation between nitrogen content and photosynthetic pigment content in crop leaves was found [40]. Therefore, nitrogen fertilizer could promote the accumulation of chlorophyll by increasing the nitrogen content of crop leaves, thus improving the photosynthetic rate of leaves. However, the sensitive bands found in the above studies were inconsistent with this study. The sensitive spectral indices of this study were ρ_{nir}, H_{500nm}, H_{675nm}, F_{710nm}, λ_{710nm}, S_{730nm}, and λ_{730nm} due to the influence of salinized soil. Hyperspectral estimation of physiological parameters of sweet corn and other crops showed that the chlorophyll absorption reflectance index (CARI), double difference index (DD), red edge inflection point (REIP), and chlorophyll red edge (CIred-edge) were good predictors of the physiological parameters, confirming the key role of the red edge spectral region [41]. Compared with the above study, the spectral index was not constructed in this study. However, many spectral transformation methods could effectively express the relationship between the spectral reflectance and biochemical components (such as chlorophyll, nitrogen content, and water status) of crops. Due to the effect of nitrogen fertilizer, many physiological and biochemical components in crops could be changed. The accuracy of the estimation model could be improved by fusing some related physiological and biochemical components with hyperspectral parameters to estimate chlorophyll, nitrogen, and other indicators [42]. Additionally, an effective method is to study the spectral characteristics of the physiological components containing nitrogen in crops. Due to the different methods used for selecting sensitive parameters, the sensitive spectral index screened in this study is rarely used as a modeling factor for estimating the physiological and biochemical components of crops.

4.2. Spectral Characteristics of the Cotton Leaves at Different Growth Stages

The content of physiological and biochemical components of plants is different in different growth stages. Due to the different contents of biochemical components in plants at different growth stages, the spectral characteristics are different. Therefore, it is of great significance to study the spectral variation characteristics of plants at different growth stages to understand the nutrient supply of plants at different stages. The results showed that the spectral characteristics of wheat were significantly affected by water stress at different growth stages [43]. Canopy chlorophyll density is a key indicator of crop growth. Xing et al. [44] showed that the spectral factors sensitive to chlorophyll density were different in different growth stages of crops. The bud stage is the fastest-growing period of cotton; however, the spectral characteristics of the cotton bud stage are rarely studied. In our study, the spectral parameters (ρ_{nir}, H_{500nm}, H_{675nm}, F_{710nm}, S_{690nm}, S_{730nm}) of the cotton bud stage increased with increasing chlorophyll density to a certain extent. In contrast to this study, Wang et al. [12] found spectral bands sensitive to oxidase activity in the cotton bud stage. Priya & Ghosh [45] studied the spectral characteristics of lead stress at different growth stages of cotton and found that the third decomposition layer between 651 nm and 742 nm after the spectral curve was transformed by wavelet; due to the stress of Pb, a significant correlation was observed above—0.70. Due to different research purposes

or processing methods of spectral data, the spectral sensitive parameters obtained were also different; however, the spectral characteristics of cotton were different in different growth stages, and the influence degree of environmental factors on spectral reflectance was not consistent in different growth stages. Because spectral reflectance is affected by many factors, which increases the complexity and uncertainty of spectral preprocessing, the method in this study is inevitably limited in application.

4.3. Influence of the Different Spectral Factors on Modeling Accuracy

If the modeling method is the same, then the selection of modeling factors is critical. The accuracy of the model is directly related to the choice of modeling factors. Nine wavelengths of 455, 545, 571, 615, 641, 662, 706, 728, and 756 nm were extracted as sensitive wavelengths; these wavelengths had a good correlation with the chlorophyll content of winter wheat [46]. Li et al. [47] compared the leaf chlorophyll content estimation accuracy of IPRF-based and NPRF-based methods and found that NpRF increased the number of frequency bands for estimating leaf chlorophyll content. Some studies showed that DCNI I was the best spectral index to estimate chlorophyll content, and PPR/NDVI was positively correlated with chlorophyll content. The combination of DCNI I and PPR/NDVI with nitrogen-related indices had good potential to evaluate nitrogen content [48]. In contrast to the above studies, part of the waveband information of the original waveband, first derivative, second derivative, and continuum removal were extracted as modeling factors in our study, and the obtained model could accurately predict the leaf chlorophyll density at the bud stage of cotton. Different spectral transformation methods could enhance the hyperspectral characteristic information, strengthen the correlation between hyperspectral reflectance and crop chlorophyll content, and improve the accuracy of the inversion model [49]. Therefore, the characteristic bands or parameters that were highly correlated with cotton chlorophyll content and came from different spectral transformation data could be selected as modeling factors to improve the stability and robustness of the model. The spectral index of different transformation methods potentially contained more useful spectral information related to chlorophyll content, which could increase the accuracy of the spectral monitoring of the chlorophyll content.

5. Conclusions

In this study, cotton leaf reflectance spectral curves and chlorophyll density data of cotton leaves with different nitrogen application rates were obtained through cotton pot experiments with different nitrogen application rates. The spectral change characteristics of cotton leaves with increasing nitrogen application rates were analyzed. The results showed the following:

(1) In the reflectance spectral curve of the cotton bud stage, the position of the near infrared reaching the platform region was consistent, which was 763 nm, and did not change with an increasing nitrogen application rate. The average reflectance at 765~880 nm was significantly different between N-stressed and N-unstressed cotton.
(2) In the continuum removal spectrum of the cotton bud stage, with increasing N application, the lowest point of the absorption valley near 500 nm shifted to the shortwave direction.
(3) The average reflectance of the near-infrared band, the absorption valley depths near 500 nm and 675 nm, the first derivative of the 710 nm reflectance, and the second derivatives of the 690 nm and 730 nm reflectance increased with increasing nitrogen application and chlorophyll density, and significant correlations were observed with the chlorophyll density.
(4) SVR and ANN algorithms were used to estimate the chlorophyll density. The results showed that the ANN algorithm could accurately predict the chlorophyll density of cotton leaves at the bud stage.

Author Contributions: Conceptualization, J.W. and W.L.; investigation, C.Y. and W.X.; methodology, J.W.; formal analysis, J.W.; resources, W.L.; writing—original draft, J.W.; writing—review and editing, S.N.; funding acquisition, W.L. and W.X. All authors have read and agreed to the published version of the manuscript.

Funding: This research was supported by grants from the National Natural Science Foundation of China (Grant No. 32360289), the Project of Xinjiang Production and Construction Corps for Scientific and Technological Innovative Talents (2022CB001-07), the Special Project for Scientific and Technological Development of Xinjiang Production and Construction Corps (2021BB024), the Science and Technology Project of Xinjiang Production and Construction Corps (2021DB019), and the Tarim University President's Fund (Grant No. TDZKSS202211).

Data Availability Statement: The datasets used in the current study are available from the corresponding author upon request.

Conflicts of Interest: The authors declare no conflicts of interest.

References

1. Najm, A.A.; Hadi, M.R.H.S.; Fazeli, F.; Darzi, M.T.; Rahi, A. Effect of Integrated Management of Nitrogen Fertilizer and Cattle Manure on the Leaf Chlorophyll, Yield, and Tuber Glycoalkaloids of Agria Potato. *Commun. Soil Sci. Plant Anal.* **2012**, *43*, 912–923. [CrossRef]
2. Gholizadeh, A.; Saberioon, M.; Borůvka, L.; Wayayok, A.; Mohd Soom, M.A. Leaf chlorophyll and nitrogen dynamics and their relationship to lowland rice yield for site-specific paddy management. *Inf. Process. Agric.* **2017**, *4*, 259–268. [CrossRef]
3. Esfahani, M.; Abbasi, H.R.A.; Rabiei, B.; Kavousi, M. Improvement of Nitrogen Management in Rice Paddy Fields Using Chlorophyll Meter (SPAD). *Paddy Water Environ.* **2008**, *6*, 181–188. Available online: https://link.springer.com/article/10.1007/s10333-007-0094-6 (accessed on 22 February 2024). [CrossRef]
4. Xiong, D.; Chen, J.; Yu, T.; Gao, W.; Ling, X.; Li, Y.; Peng, S.; Huang, J. SPAD-based leaf nitrogen estimation is impacted by environmental factors and crop leaf characteristics. *Sci. Rep.* **2015**, *5*, 13389. [CrossRef] [PubMed]
5. Ata-Ul-Karim, S.T.; Cao, Q.; Zhu, Y.; Tang, L.; Rehmani MI, A.; Cao, W. Non-destructive assessment of plant nitrogen parameters using leaf chlorophyll measurements in rice. *Front. Plant Sci.* **2016**, *7*, 1829. [CrossRef] [PubMed]
6. Kaivosoja, J.; Pesonen, L.; Kleemola, J.; Plnen, I.; Rajala, A. A case study of a precision fertilizer application task generation for wheat based on classified hyperspectral data from UAV combined with farm history data. *Remote Sens. Agric. Ecosyst. Hydrol. XV* **2013**, *8887*, 118–127. [CrossRef]
7. Ranghetti, M.; Boschetti, M.; Ranghetti, L.; Tagliabue, G.; Panigada, C.; Gianinetto, M.; Verrelst, J.; Candiani, G. Assessment of maize nitrogen uptake from PRISMA hyperspectral data through hybrid modelling. *Eur. J. Remote Sens.* **2023**, *56*, 2117650. [CrossRef] [PubMed]
8. Gopinath, G.; Surendran, U.; Vishak, J.; Sasidharan, N.; CT, M.F. Hyperspectral data and vegetative indices for paddy: A case study in Kerala, India. *Remote Sens. Appl. Soc. Environ.* **2024**, *33*, 101109. [CrossRef]
9. Liu, S.; Li, L.; Fan, H.; Guo, X.; Wang, S.; Lu, J. Real-time and multi-stage recommendations for nitrogen fertilizer topdressing rates in winter oilseed rape based on canopy hyperspectral data. *Ind. Crops Prod.* **2020**, *154*, 112699. [CrossRef]
10. Zhang, H.; Lan, Y.; Suh, C.P.; Westbrook, J.K.; Lacey, R.; Hoffmann, W.C. Differentiation of cotton from other crops at different growth stages using spectral properties and discriminant analysis. *Trans. ASABE* **2012**, *55*, 1623–1630. [CrossRef]
11. Ma, Y.; Zhang, Q.; Yi, X.; Ma, L.; Zhang, L.; Huang, C.; Zhang, Z.; Lv, X. Estimation of Cotton Leaf Area Index (LAI) Based on Spectral Transformation and Vegetation Index. *Remote Sens.* **2022**, *14*, 136. [CrossRef]
12. Wang, J.; Tian, T.; Wang, H.; Cui, J.; Zhu, Y.; Zhang, W.; Tong, X.; Zhou, T.; Yang, Z.; Sun, J. Estimating cotton leaf nitrogen by combining the bands sensitive to nitrogen concentration and oxidase activities using hyperspectral imaging. *Comput. Electron. Agric.* **2021**, *189*, 106390. [CrossRef]
13. Li, L.; Li, F.; Liu, A.; Wang, X. The prediction model of nitrogen nutrition in cotton canopy leaves based on hyperspectral visible-near infrared band feature fusion. *Biotechnol. J.* **2023**, *18*, e2200623. [CrossRef] [PubMed]
14. Chen, X.; Lv, X.; Ma, L.; Chen, A.; Zhang, Q.; Zhang, Z. Optimization and validation of hyperspectral estimation capability of cotton leaf nitrogen based on SPA and RF. *Remote Sens.* **2022**, *14*, 5201. [CrossRef]
15. Prananto, J.A.; Minasny, B.; Weaver, T. Rapid and cost-effective nutrient content analysis of cotton leaves using near-infrared spectroscopy (NIRS). *PeerJ* **2021**, *9*, e11042. [CrossRef]
16. Dedeoğlu, M. Estimation of critical nitrogen contents in peach orchards using visible-near infrared spectral mixture analysis. *J. Near Infrared Spectrosc.* **2020**, *28*, 315–327. [CrossRef]
17. Yi, Q.; Wang, F.; Bao, A.; Jiapaer, G. Leaf and canopy water content estimation in cotton using hyperspectral indices and radiative transfer models. *Int. J. Appl. Earth Obs. Geoinf.* **2014**, *33*, 67–75. [CrossRef]
18. Zhang, L.; Zhou, Z.; Zhang, G.; Meng, Y.; Chen, B.; Wang, Y. Monitoring the leaf water content and specific leaf weight of cotton (*Gossypium Hirsutum* L.) in saline soil using leaf spectral reflectance. *Eur. J. Agron.* **2012**, *41*, 103–117. [CrossRef]

19. Feng, D.; Xu, W.; He, Z.; Zhao, W.; Yang, M. Advances in plant nutrition diagnosis based on remote sensing and computer application. *Neural Comput. Appl.* **2020**, *32*, 16833–16842. [CrossRef]
20. Heng, T. Accumulation Characteristics and Optimal Regulation of Water, Salt and Nutrient in Film−Mulched Cotton (*Gossypium Hirsutum* L.) and Nutrient in Film−Mulched Cotton (*Gossypium Hirsutum* L.). Doctoral Dissertation, Shihezi University, Xinjiang, China, 2022. (In Chinese) [CrossRef]
21. Han, Q.; Xue, L.; Qi, T.; Liu, Y.; Yang, M.; Chu, X.; Liu, S. Assessing the impacts of future climate and land-use changes on streamflow under multiple scenarios: A case study of the upper reaches of the Tarim River in northwest China. *Water* **2024**, *16*, 100. [CrossRef]
22. Zebarth, B.J.; Younie, M.; Paul, J.W.; Bittman, S. Evaluation of leaf chlorophyll index for making fertilizer nitrogen recommendations for silage corn in a high fertility environment. *Commun. Soil Sci. Plant Anal.* **2002**, *33*, 665–684. [CrossRef]
23. Khosravi, V.; Ardejani, F.D.; Yousefi, S.; Aryafar, A. Monitoring soil lead and zinc contents via combination of spectroscopy with extreme learning machine and other data mining methods. *Geoderma* **2018**, *318*, 29–41. [CrossRef]
24. Que, H.; Zhao, X.; Sun, X.; Zhu, Q.; Huang, M. Identification of wheat kernel varieties based on hyperspectral imaging technology and grouped convolutional neural network with feature intervals. *Infrared Phys. Technol.* **2023**, *131*, 104653. [CrossRef]
25. Burket, M.O.; Olmanson, L.G.; Brezonik, P.L. Comparison of Two Water Color Algorithms: Implications for the Remote Sensing of Water Bodies with Moderate to High CDOM or Chlorophyll Levels. *Sensors* **2023**, *23*, 1071. [CrossRef] [PubMed]
26. Flynn, K.C.; Baath, G.; Lee, T.O.; Gowda, P.; Northup, B. Hyperspectral reflectance and machine learning to monitor legume biomass and nitrogen accumulation. *Comput. Electron. Agric.* **2023**, *211*, 107991. [CrossRef]
27. Wang, J.; Ding, J.; Yu, D.; Teng, D.; He, B.; Chen, X.; Ge, X.; Zhang, Z.; Wang, Y.; Yang, X.; et al. Machine learning-based detection of soil salinity in an arid desert region, Northwest China: A comparison between Landsat-8 OLI and Sentinel-2 MSI. *Sci. Total Environ.* **2020**, *707*, 136092. [CrossRef] [PubMed]
28. Kesteven, G. The coefficient of variation. *Nature* **1946**, *158*, 520–521. [CrossRef]
29. Tian, T.; Wang, J.; Wang, H.; Cui, J.; Shi, X.; Song, J.; Li, T.; Li, W.; Zhong, M. Synergistic use of spectral features of leaf nitrogen and physiological indices improves the estimation accuracy of nitrogen concentration in rapeseed. *Int. J. Remote Sens.* **2022**, *43*, 2755–2776. [CrossRef]
30. Kang, J.; Chu, Y.; Ma, G.; Zhang, Y.; Zhang, X.; Wang, M.; Lu, H.; Wang, L.; Kang, G.; Ma, D.; et al. Physiological mechanisms underlying reduced photosynthesis in wheat leaves grown in the field under conditions of nitrogen and water deficiency. *Crop J.* **2023**, *11*, 638–650. [CrossRef]
31. Wang, H.; Wu, L.; Cheng, M.; Fan, J.; Zhang, F.; Zou, Y.; Chau, H.W.; Gao, Z.; Wang, X. Coupling effects of water and fertilizer on yield, water and fertilizer use efficiency of drip-fertigated cotton in northern Xinjiang, China. *Field Crops Res.* **2018**, *219*, 169–179. [CrossRef]
32. Ali, S.; Hafeez, A.; Ma, X.; Tung, S.A.; Chattha, M.S.; Shah, A.N.; Luo, D.; Ahmad, S.; Liu, J.; Yang, G. Equal potassium-nitrogen ratio regulated the nitrogen metabolism and yield of high-density late-planted cotton (*Gossypium hirsutum* L.) in Yangtze River valley of China. *Ind. Crops Prod.* **2019**, *129*, 231–241. [CrossRef]
33. Li, L.; Wang, Y. Independent and combined influence of drought stress and nitrogen deficiency on physiological and proteomic changes of barley leaves. *Environ. Exp. Bot.* **2023**, *210*, 105346. [CrossRef]
34. Fiorio, P.R.; José, A.M.D.; Nanni, M.R.; Formaggio, A.R. Spectral differentiation among soils using spectral data from laboratory and orbital sensor. *Bragantia* **2009**, *69*, 453–466. [CrossRef]
35. Prsa, I.; Stampar, F.; Vodnik, D.; Veberic, R. Influence of nitrogen on leaf chlorophyll content and photosynthesis of 'Golden Delicious' apple, Acta Agriculturae Scandinavica. *Sect. B Soil Plant Sci.* **2007**, *57*, 283–289. [CrossRef]
36. Liu, K.; Chen, Y.; Li, S.; Wang, W.; Zhang, W.; Zhang, H.; Gu, J.; Yang, J.; Liu, L. Differing responses of root morphology and physiology to nitrogen application rates and their relationships with grain yield in rice. *Crop J.* **2023**, *11*, 618–627. [CrossRef]
37. Yang, Y.; Huang, Z.; Wu, Y.; Wu, W.; Lyu, L.; Li, W. Effects of nitrogen application level on the physiological characteristics, yield and fruit quality of blackberry. *Sci. Hortic.* **2023**, *313*, 111915. [CrossRef]
38. Marlene, B.H.S.; Onécimo, G.J.; Manuel SH, Á.; Iván, G.V.R.; Jairo, D.R.; Manelik, G.L.A.; Roberto, S.; Daniel, G.M.; David, I.G.R.; Francisco, D.M.R.; et al. Effects of Different Irrigation Regimes and Nitrogen Fertilization on the Physicochemical and Bioactive Characteristics of onion (*Allium cepa* L.). *Horticulturae* **2023**, *9*, 344. [CrossRef]
39. Han, P.; Zhai, Y.; Liu, W.; Lin, H.; An, Q.; Zhang, Q.; Ding, S.; Zhang, D.; Pan, Z.; Nie, X. Dissection of hyperspectral reflectance to estimate photosynthetic characteristics in upland cotton (*Gossypium Hirsutum* L.) under different nitrogen fertilizer application based on machine learning algorithms. *Plants* **2023**, *12*, 455. [CrossRef] [PubMed]
40. Kubar, M.S.; Wang, C.; Noor, R.S.; Feng, M.; Yang, W.; Kubar, K.A.; Soomro, K.; Yang, C.; Sun, H.; Mohamed, H.; et al. Nitrogen fertilizer application rates and ratios promote the biochemical and physiological attributes of winter wheat. *Front. Plant Sci.* **2022**, *13*, 1011515. [CrossRef] [PubMed]
41. Sellami, M.H.; Albrizio, R.; Čolović, M.; Hamze, M.; Cantore, V.; Todorovic, M.; Piscitelli, L.; Stellacci, A.M. Selection of Hyperspectral Vegetation Indices for Monitoring Yield and Physiological Response in Sweet Maize under Different Water and Nitrogen Availability. *Agronomy* **2022**, *12*, 489. [CrossRef]
42. Tian, T.; Wang, J.; Wang, H.; Cui, J.; Shi, X.; Song, J.; Li, W.; Zhong, M.; Qiu, Y.; Xu, T. Nitrogen application alleviates salt stress by enhancing osmotic balance, ROS scavenging, and photosynthesis of rapeseed seedlings (*Brassica napus*). *Plant Signal Behav* **2022**, *17*, 2081419. [CrossRef]

43. Li, Q.; Gao, M.; Li, Z. Ground Hyper-Spectral Remote-Sensing Monitoring of Wheat Water Stress during Different Growing Stages. *Agronomy* **2022**, *12*, 2267. [CrossRef]
44. Xing, N.; Huang, W.; Ye, H.; Dong, Y.; Kong, W.; Ren, Y.; Xie, Q. Remote sensing retrieval of winter wheat leaf area index and canopy chlorophyll density at different growth stages. *Big Earth Data* **2022**, *6*, 580–602. [CrossRef]
45. Priya, S.; Ghosh, R. Monitoring effects of heavy metal stress on biochemical and spectral parameters of cotton using hyperspectral reflectance. *Environ. Monit. Assess.* **2022**, *195*, 112. [CrossRef] [PubMed]
46. Zhang, Y.; Hui, J.; Qin, Q.; Sun, Y.; Zhang, T.; Sun, H.; Li, M. Transfer-learning-based approach for leaf chlorophyll content estimation of winter wheat from hyperspectral data. *Remote Sens. Environ.* **2021**, *267*, 112724. [CrossRef]
47. Li, Y.; Sun, Z.; Lu, S. Optimizing two-band spectral indices to estimate leaf chlorophyll content using the non-polarized reflectance factors. *IEEE Geosci. Remote Sens. Lett.* **2022**, *19*, 1–5. [CrossRef]
48. Jin, X.; Li, Z.; Feng, H.; Xu, X.; Yang, G. Newly combined spectral indices to improve estimation of total leaf chlorophyll content in cotton. *IEEE J. Sel. Top. Appl. Earth Obs. Remote Sens.* **2014**, *7*, 4589–4600. [CrossRef]
49. Shi, H.; Guo, J.; An, J.; Tang, Z.; Wang, X.; Li, W.; Zhao, X.; Jin, L.; Xiang, Y.; Li, Z.; et al. Estimation of chlorophyll content in soybean crop at different growth stages based on optimal spectral index. *Agronomy* **2023**, *13*, 663. [CrossRef]